Chapter 12

RIBOSOMAL CRYSTALLOGRAPHY: DYNAMICS, FLEXIBILITY AND PEPTIDE BOND FORMATION

Ada Yonath*

High-resolution crystal structures of functionally active ribosomal particles provide unique tools for understanding key questions concerning ribosomal function, mobility, dynamics, and involvement in cellular regulation. Structure analysis of complexes of ribosomal particles with substrate analogs and universal drugs indicated that ribosomes provide the structural frame for precise positioning of the tRNA molecules rather than participate in the catalytic event, and that the peptide bond is being formed by a nucleophilic attack of the amino moiety of the residue bound to A-site tRNA on the carbonyl carbon at the P-site. Clinically relevant antibiotics interact almost exclusively with rRNA. They interfere with substrate binding, limit the conformational mobility, block the nascent chain exit tunnel or hinder the progression of growing peptide chains.

Keywords: Protein synthesis, ribosomes, translation factors, GTP hydrolysis, L12.

INTRODUCTION

In rapidly growing cells, the compounds involved in the translation of the genetic code into proteins constitute about half of the cell's dry weight and consumes up to 80% of the cell's energy. This fundamental life process involves the participation of more than a hundred components; among them is the ribosome, the largest known macromolecular enzyme.

*Department of Structural Biology; Weizmann Institute of Science, 76100 Rehovot Israel Email address: yonath@mpgars.desy.de

Ribosomes are the universal cellular organelles built of two subunits of unequal size. The prokaryotic ribosomal small subunit (called 30S) has a molecular weight of 8.5×10^5 Dalton and contains one RNA chain of over 1500 nucleotides and 20 proteins. The prokaryotic large ribosomal subunit (called 50S) is of molecular weight of 1.5×10^6 Dalton and contains two RNA chains with a total of about 3000 nucleotides and around 35 proteins.

The smaller subunit has key roles in the initiation of the translation process, in decoding the genetic message, in discriminating against non- and near-cognate amino-acylated tRNA molecules, and in controlling the fidelity of codon-anticodon interactions. The larger subunit contains the peptidyl transferase center, the site where the peptide bonds are created. Upon initiation of protein synthesis, the two ribosomal subunits associate to form functionally active 70S ribosome, utilizing amino acids brought to it by amino-acylated tRNA molecules. Within the ribosome there are three binding sites for transfer RNA (tRNA), designated the P (peptidyl), A (aminoacyl) and E (exit) sites which are partly located on both the small and the large subunits. The anticodon loops of the three tRNA molecules bind to the small subunit, whereas the acceptor stems bind to the large subunit. Both subunits work together to translocate all three tRNAs molecules and the associated mRNA chain by precisely one codon with respect to the ribosome. The entire process depends on an energy source, the hydrolysis of GTP, and several extrinsic cellular protein factors.

The ribosome is a precisely engineered molecular machine that performs an intricate multi-step process that requires smooth and rapid switches between different conformations. Both ribosomal subunits can undergo reversible alterations and contain structural elements that participate in global motions together with local rearrangements. One of the major events involved in protein biosynthesis that requires significant mobility of both ribosomal subunits is the GTPase-dependent translocation. In the course of protein biosynthesis, once a peptide bond is formed, the P-site tRNA is deacylated and its acceptor end moves to the E (exit)-site, while the A-site tRNA, carrying the nascent chain moves into the P-site. This fundamental act in the elongation cycle of protein synthesis is

called translocation. It may be performed either by a simple translation of entire tRNA molecules, according to the classical three-site model (Rheinberger *et al*., 1981, Lill and Wintermeyer, 1987), or incorporate an additional intermediate hybrid state. According to the latter proposal, translocation occurs in two discrete steps. In the first, spontaneous step, that occurs right after peptide bond formation, the tRNA acceptor end moves relative to the large subunit. In the second step, which is promoted by EF-G, the anticodon moves relative to the small subunit (Moazed and Noller, 1989, Wilson and Noller, 1998).

Antibiotics are natural or man-made compounds, designed to interfere with bacterial metabolism and eliminate bacteria by inhibiting the biosynthesis of protein or DNA or cell-wall components. About 40% of the known antibiotics interfere with protein biosynthesis. The ribosome is one of the main binding targets for a broad range of natural and synthetic antibiotics. Structurally diverse natural as well as synthetic compounds efficiently inhibit ribosomal function (Cundliffe, 1981, Spahn and Prescott, 1996). Theoretically the ribosome offers multiple opportunities for the binding of small compounds, but practically all the known drugs utilize only a few sites. Biochemical information about binding and action of antibiotics on the ribosome has been accumulated for almost four decades.

Puromycin played a central role in biochemical experiments aimed at the understanding of the mechanism of peptide bond formation (Pestka, 1977, Vazquez, 1979, Gale *et al*., 1981, Porse and Garrett, 1995, Rodriguez-Fonseca *et al*., 2000) since it can bind to the A-site (Moazed and Noller, 1991, Monro *et al*., 1969, Smith *et al*., 1965, Traut and Monro, 1964) as well as to the P-site, albeit to a lower extent (Bourd *et al*., 1983, Kirillov *et al*., 1997). Puromycin, which was named "antibiotic agent" because it is a product of a microorganism, is a universal ribosome inhibitor, since it binds to all ribosomes. It binds at the peptidyl transferase center (Rodriguez-Fonseca *et al*., 2000) and as such is being used for studies on the mechanism of peptide bond formation. Unlike other antibiotics, puromycin does not lead to drug-resistance by mutations in the PTC (Garrett and Rodriguez-Fonseca, 1995). Puromycin is partially costructural with the 3' terminus of aminoacyl-tRNA (Harms *et al*., 2001), but its aminoacyl residue is linked via an amide bridge rather than an

ester bond. Puromycin is known to bind weakly to the large subunit and a high concentration of methanol or ethanol, is required to enhance its binding. Puromycin probing in the presence of an active donor substrate can result in peptide bond formation (Odom *et al*., 1990), which is uncoupled from movement of the A-site tRNA (Green *et al*., 1998). No further synthesis can take place since the amide bond of puromycin cannot be cleaved; hence the peptidyl-puromycin so obtained falls off the ribosome.

Among the antibiotics that target ribosomes, the macrolides have the highest clinical usage. They act against gram-positive aerobes and some gram-negative aerobes. Most macrolides have a broad-spectrum antimicrobial activity and are used primarily for respiratory, skin and soft tissue infections. The macrolide family is large and structurally diverse. The central component of the macrolides is a lactone ring. The 14-member ring macrolides are among the most important antibiotics. Better stability and improved spectrum of activity characterize Macrolides of the second generation, such as chlarithromycin or roxithromycin. Subsequent rapid spread of antibiotic-resistant strains has stimulated the search for additional novel derivatives. The macrolides of the third generation, the ketolides, show an improved activity profile, and are more active against certain macrolide-resistant strains.

The high-resolution structures of the two ribosomal subunits form eubacteria were found suitable to serve as pathogen-models. Using them as references allowed unambiguous localization of over a dozen antibiotic drugs, most of which are clinically relevant antibiotics (Brodersen *et al*., 2000, Carter *et al*., 2000, Pioletti *et al*., 2001, Schluenzen *et al*., 2001, Hansen *et al*., 2002). Co-crystals were grown, each containing a complex of one of the ribosomal subunits and an antibiotic agent at a clinically relevant concentration. Alternatively, crystals of ribosomal particles were soaked in solutions containing antibiotics at clinically relevant concentrations. In most cases the co-crystals of antibiotics and the ribosomal subunits yielded crystallographic data of quality that was sometimes better than that obtained from crystals of free particles (Carter *et al*., 2000, Schluenzen *et al*., 2001), presumably because the antibiotics reduce internal motions of flexible regions and increase homogeneity.

Analysis of the structures of the antibiotics complexes showed diversity in the antibiotics modes of action, such as interference with substrate binding, hindrance of the mobility required for the biosynthetic process and the blockage of tunnel which provides the path of the nascent proteins. Most of the antibiotics studied by us were found to bind primarily to ribosomal RNA and, except for two that caused allosteric effects; their binding did not cause major conformational changes.

SOME HISTORICAL COMMENTS

High-resolution crystal structures of ribosomal particles and of their complexes with substrate analogues, inhibitors and antibiotics, currently emerging in an impressive speed, led to a quantum jump in our understanding of the translation process. These studies were idealized over two decade ago (Yonath *et al*., 1980) once we established that the key to high-resolution data is to crystallize highly active homogenous preparations of robust ribosomal particles under conditions similar to their *in-situ* environments and to minimize crystal heterogeneity by inducing selected conformations within the crystals. An alternative approach is to design complexes containing ribosomes at defined functional stages, such as of the entire ribosome with tRNA and mRNA molecules (Hansen *et al*., 1990). This approach was later adopted, refined and extended, and has led a medium resolution structure of the ribosome with three tRNA molecules (Yusupov *et al*., 2001).

Robust ribosomal particles were chosen assuming that they would maintain their integrity during preparation, hence should provide suitable material for crystallization. We focused on thermophilic bacteria, *Bacillus stearothermopilus* and *Thermus thermophilus;* as well as on *Haloarcula marismortui,* the bacterium leaving in the Dead-Sea, the lake of the highest salinity worldwide. The recent addition is *Deinococcus radiodurans,* an extremely robust gram-positive mesophilic eubacterium with a ribosome that shares extensive similarity the ribosomes of *Escherichia coli* and *T. thermophilus*. This species was originally identified as a contaminant of irradiated canned meat, and later isolated from environments that are either very rich or extremely poor in organic nutrients, ranging from soil and animal feces to weathered granite in a dry Antarctic valley,

room dust, wastes of atomic-piles and irradiated medical instruments. It also is the organism with the highest level of radiation-resistance currently known. It survives under conditions that cause DNA damage, such as hydrogen peroxide, and ionizing or ultraviolet radiation. It contains systems for DNA repair, DNA damage export, desiccation, starvation recovery and genetic redundancy (White *et al*., 1999).

The first crystals that yielded some crystallographic information were grown from of the large subunit from *B. stearothermophilus* (Yonath *et al*., 1980, Yonath *et al*., 1984). The large ribosomal subunit from *H. marismortui* (Shevack *et al*., 1985) yielded, after a few years, high-resolution diffraction (Makowski *et al*., 1987, von Bohlen *et al*., 1991). Crystals of the large and small subunits from *T. thermophilus,* T50S (Muessig *et al*., 1989, Volkmann *et al*., 1990) and T30S (Yonath *et al*., 1988), respectively, diffracting to low resolution were grown in parallel. Microcrystals of the latter were obtained also by the Russian group headed by A. Spirin and B. Weinstein (Trakhanov *et al*., 1987).

The crystals of the large ribosomal subunit from *D. radiodurans* and of their complexes with antibiotics and substrate analogs that were grown and kept under conditions almost identical to those optimized for maximizing their biological activity (Schluenzen *et al*., 2001, Harms *et al*., 2001). These crystals were found to provide an excellent system to investigate the peptide bond formation (Bashan *et al*., 2002) to gain more insight into functional flexibility (Yonath, 2002, Zarivach *et al*., 2002) to extend the information of antibiotics binding towards rational drug design; to identify the exit tunnel gate and reveal the structural basis for the involvement of the ribosome in cellular regulation (Berisio *et al*., 2002).

Over the years it was found that all ribosomal crystals present challenging technical problems, owing to their enormous size; their complexity; their natural tendency to deteriorate and disintegrate; their internal flexibility and their extreme sensitivity to irradiation. Assuming that one of the main reasons for crystal decay is the progression of free radicals that are produced by the X-ray beam, we pioneered crystallographic data collection at cryogenic temperature (Hope *et al*., 1989, Yonath *et al*., 1987a). This procedure was found to minimize dramatically the harm caused by irradiation, and therefore became rapidly the routine way for collecting crystallographic data from biological crystals. The application

of cryo crystallography together with the advances of the X-ray sources, namely the installation of third generation synchrotrons equipped with state-of-the-art detectors, and the increased sophistication in the phasing methods, enabled us, as well as others, to handle most of the technical problems.

THE GLOBAL ORGANIZATION OF THE TWO RIBOSOMAL SUBUNITS

The overall structures of both ribosomal subunits, as determined by us (Schluenzen *et al*., 2000, Harms *et al*., 2001) are shown in Figure 1. The two subunits differ in shape and in their global organization. Thus, whereas the small one is built of distinct structural domains, the core of the large subunit seems to be more compact. In both subunits the ribosomal RNA dominates most of the ribosome structure. We placed mRNA and tRNA in the ribosomal particles by reference to the structures of the complex of the entire ribosome with three tRNA molecules that were determined at 5.5 Å resolution (Yusupov *et al*., 2001). This placement reconfirmed that the anticodon loops of the A- and P-site tRNAs as well as the mRNA do not contact any ribosomal proteins.

Common to both subunits are the overall structures of the ribosomal proteins and their distribution. Almost all ribosomal proteins contain long tails or extended internal loops. In general, the globular domains are peripheral, located on the particle's surface, at its solvent side. The involvement of proteins in the stabilization of the structure is achieved mainly through their long extensions that penetrate into rRNA regions and serve as molecular linkers, struts and supports, as observed in viruses (Huang *et al*., 1998). Another group of proteins have tails pointing towards the solution, similar to their positioning in the nucleosome (Luger *et al*., 1997), presumably acting as tentacles that enhance the binding of non ribosomal compounds that attach to the ribosome.

A few proteins do not have extensions, are built of more than a single globular domain. These are located either at the ends of functionally important protuberances (L1, L7/L12, L10, L11) or fill a gap between the

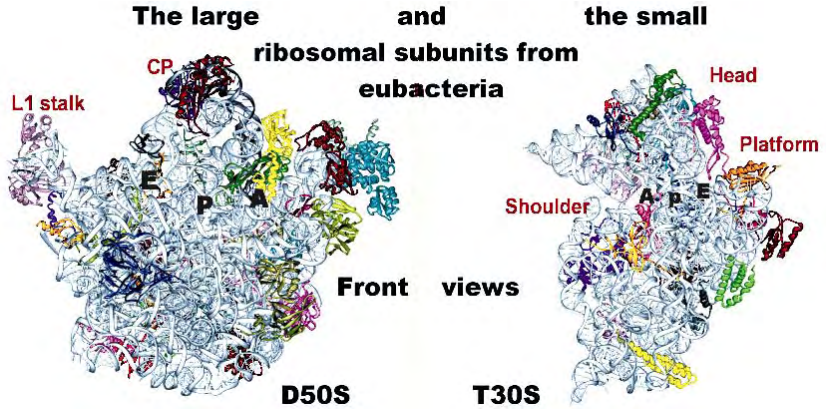

Fig. 1. The "front views" (interfaces) of the two ribosomal subunits from eubacteria. A, P, and E, designate the sites of the interactions of the three tRNA with the small subunit (their anticodon loops with the decoding region), and with the large subunit (at their elbows).

central protuberance and one of the stalks (Harms *et al*., 2001). Most of the globular domains of the proteins are located at the periphery and their long tails that penetrate into the RNA core are believed to stabilize its structure. Protein tails that point into the solution, may act as tentacles for enhancing the binding of non-ribosomal factors participating in protein biosynthesis (Gluehmann *et al*., 2001, Pioletti *et al*., 2001, Zarivach *et al*., 2002). The striking architecture of the ribosome allows for substantial domain mobility. Yet, the individual structural elements are rather stable. The features that contribute to the local stability include specific RNA folds, by a high G-C content at the rims of strategically located junctions and by the ribosomal proteins.

The Small Ribosomal Subunit

The high-resolution structure of the small subunit from *Thermus thermophilus* has been determined by us (Schluenzen *et al*., 2000, Pioletti *et al*., 2001) and by the group of V. Ramakrishnan at MRC, UK (Wimberly *et al*., 2000). The emerging particles from both electron density maps are similar and contain the morphological features familiar from early electron microscopy studies (Lake, 1985, Stoffler and Stoffler-Meilicke, 1984). The main structural features of this subunit, the "head", "neck"

and "body" that contains a "shoulder" and a "platform", radiate from the junction combining the head and the body (Figure 2), a location that hosts the decoding center.

The principal component of the subunit interface region is the long penultimate helix (H44), which is responsible for most of the contacts with the larger subunit within the ribosome. It consists of over a 100 nucleotides, of which the only evolutionarily conserved part comprising of less than two dozen nucleotides that are involved in decoding and in P-site tRNA binding. Helix H44 is one of three long helices run parallel to the vertical axis of the body, likely to transmit structural rearrangements, correlating events at the particle's far ends with the cycle of mRNA translocation at the decoding region. Transverse features, placed like ladder rungs between them, link the three longitudinal helices. Principal among these transverse helices is an inclined lune extending from the shoulder to the platform. The head contains most of the 3' region of the 16S RNA, arranged mainly in short helices, in marked contrast to the long features of the body. The head has a bi-lobal architecture, with a longer helix (H34) serving as the bridge between hemispheres. It joins the body through a slender connection, made of a single RNA helix which appears to act as a hinge while translocation.

The shoulder plays a key role in mRNA binding, as it forms the lower side of an elongated, curved channel, which we assigned as entrance side of the path of the mRNA. A latch (Schluenzen *et al*., 2000), which can be described as a non-covalent body-head connection, is formed by the shoulder and the lower part of the head, is the feature that designates the entrance to the mRNA channel. This latch facilitates mRNA threading and provides the special geometry that guarantees processivity and ensures maximized fidelity. It controls the entrance to the mRNA channel by creating a pore of varying diameter and its relative location may be dictated by the head twist.

The decoding region contains features from the upper part of the body and the lower part of the head. Mapping the conserved nucleotides in the 16S RNA on our structure showed remarkable conservation around this region, in accord with the universality of the decoding process. The

most prominent feature in the decoding center is the upper portion of H44, which bends towards the neck and forms most of the intersubunit contacts in the assembled ribosome (Yusupov *et al*., 2001). Its upper bulge forms the A- and P-tRNA sites for codon-anticodon interactions. A helix, called the "switch helix" or H27, packs groove-to-groove with the upper end of H44. This helix can undergo rearrangements in its base-pairing scheme that may induce global conformational rearrangements Lodmell and Dahlberg, 1997).

The Large Ribosomal Subunit

The availability of two high-resolution crystal structures of unbound large ribosomal subunits, the archaeal H50S (Ban *et al*., 2000) and eubacterial D50S (Harms *et al*., 2001), as well as a lower resolution structure of T50S within the T70S ribosome (Yusupov *et al*., 2001), provide a unique tool for comparative studies. In the particular case of H50S and D50S, such comparison should shed light on the correlation between the structure, the function and the environment, as well as on phylogenetic aspects.

Both crystal structures of the large subunit are similar to the traditional shape of the large ribosomal subunit, as seen by electron microscopy (Mueller *et al*., 2000, Penczek *et al*., 1999). This view, often referred to as the "crown view", looks like a halved pear with two lateral protuberances, called the L1 and L7/L12 stalks, is shown in Figures 1

Fig. 2. (Figure on facing page)
Top: The three-dimensional structure of T30S, emphasizing the distribution of RNA and proteins (silver: RNA, blue: proteins). Left: the interface with the large subunit. Right: Side view. Obtained by rotating the left view by 90 degrees around its long axis. The yellow circle shows the location of protein S2. Two conformations of this protein are shown in the middle. In yellow: the structure of this protein in native ribosomes, and in cyan: the structure of the tungstenated protein. The tungsten atoms bound to this protein are shown in red.
Middle right: the two orientations of the head, seen in crystals diffracting to low-resolution.
Bottom: left: the domains of the small subunit RNA are shown in different colors.
Right: the detailed view of the binding site of edeine (purple). The 30S platform is represented by two helices involved in its movement. Note the newly formed base pair in green). The docked P-site tRNA (orange) and E-site tRNA (gold) are also shown.

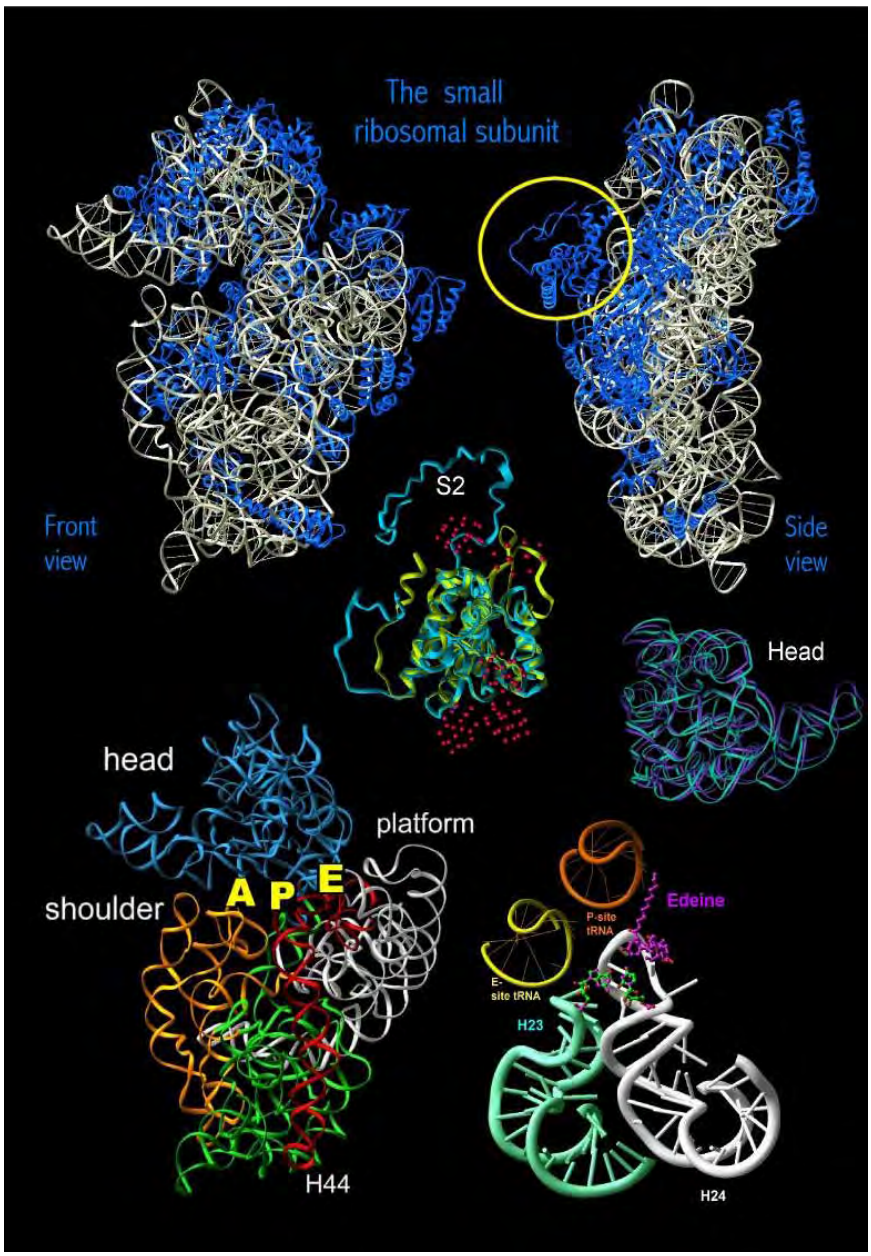
The small
ribosomal subunit
Front
view
Side
view
S2
Head
head
platform
shoulder
A P E
H44
Edeine
P-site
tRNA
E-
site tRNA
H23
H24

Fig. 2.

and 2. The core of the large ribosomal subunit is built of interwoven RNA features. Its flat surface faces the small subunit in the 70S ribosome and its round back side faces the solvent.

The gross similarity of the rRNA fold of D50S to the available 50S structures allowed superposition of the model of D50S onto that of the 2.4 Å structure of H50S (Ban *et al*., 2000) and of the 50S subunit within the 5.5 Å structure of the T70S ribosome (Yusupov *et al*., 2001). However, we detected significant structural differences even within the conserved regions, which cannot be explained solely by expected phylogenetic variations. In addition, the riboosmal proteins show remarkable differences, even when sharing homology with their counterparts in H50S. In addition, D50S contains several proteins that have no counterparts in H50S. We detected RNA segments replacing proteins and vice versa. Of structural interest is a three domains protein (CTC), alongside with an extended alpha helical protein (L20) and two Zn-finger proteins (L32 and L36).

The peptidyl transferase cavity

Peptide bond formation, the principal reaction of protein biosynthesis, has been localized in the large subunit over three decades ago (Monro *et al*., 1968, Cundliffe, 1990, Moazed and Noller, 1991, Noller *et al*., 1992, Garrett and Rodriguez-Fonseca, 1995, Samaha *et al*., 1995), in a multi branched loop in the 23S RNA. Among the 43 nucleotides forming the PT ring 36 are conserved in *H. marismortui* and *D. radiodurans.* Despite the high conservation and the wealth of information accumulated over the years and the availability of crystallographic structures, the molecular mechanism of peptidyl transferase (PT) activity is still not well understood. The only proposal for catalytic involvement of the ribosome that was based on crystal structure, proposed an acid-base catalysis (Nissen *et al*., 2000) generated doubts (Barta *et al*., 2001, Polacek *et al*., 2001, Thompson *et al*., 2001, Bayfield *et al*., 2001). As seen below, our results (Schluenzen *et al*., 2001, Harms *et al*., 2001, Yonath, 2002) support alternative suggestions, that the ribosome facilitates peptide bond formation by providing the structural frame that allows precise positioning of the tRNA molecules as well as for the generation of the energy required

for the formation of the peptide bond (Nierhaus *et al*., 1980, Samaha *et al*., 1995, Green and Noller, 1997, Pape *et al*., 1999, Polacek *et al*., 2001).

Superposition of the backbone of the structures of the PT center (PTC) in the two unbound large subunits of H50S and D50S on that of the bound large subunit within T70S, show similar, but not identical folds. The orientations of some of the nucleotides, however, show distinct differences (Yusupov *et al*., 2001, Harms *et al*., 2001). It is possible that the different orientations reflect the flexibility needed for the formation of the peptide bond. It is also possible, however, that the different orientations result from the differences in the functional states of the 50S subunit in the two crystal forms, consistent with the structural changes that were found to occur at distinct nucleotides of the peptidyl transferase ring upon transition between the active and inactive conformations through chemical probing with dimethyl sulfate (Bayfield *et al*., 2001). In support of this suggestion are experiments performed over three decades ago on the *E. coli* 50S subunits (Miskin *et al*., 1968, Vogel *et al*., 1971, Zamir *et al*., 1974), that indicated that the relative orientations of several nucleotides within the peptidyl transferase center vary upon alterations in the monovalent ion concentrations in magnitudes that are much lower than the modifications in the concentrations and types of the monovalent ions that were employed in the course of the determination of the structure of H50S (Ban *et al*., 2000).

The PTC is situated above the entrance to the polypeptide exit tunnel, a major component of the ribosome that could be detected even by conventional electron microscopy at low resolution (Milligan and Unwin, 1986, Yonath *et al*., 1987b). Despite the low resolution, these studies showed that this tunnel spans the large subunit from the location assumed to be the peptidyl transferase site to its lower part, and that it is about 100 Å in length and up to 25 Å in diameter (Yonath *et al*., 1987b), dimensions consistent with the suggestion, made more than three decades ago, that the newest synthesized part of a nascent protein is masked by the ribosome (Malkin and Rich, 1967, Sabatini and Blobel, 1970). The existence of the exit tunnel was confirmed at high resolution in H50S (Nissen *et al*., 2000) and in D50S (Harms *et al*., 2001). Based on the

structure of H50S it was suggested that the walls of the tunnel have a "nonstick" character (Nissen *et al*., 2000).

MOBILITY, FLEXIBILITY AND FUNCTIONAL ACTIVITY

From the initial stage of ribosomal crystallography our aim was to elucidate structures of ribosomal particles trapped at functionally relevant conformations. We developed two approaches: (a) crystallize and maintain the crystals under close to physiological conditions, or (b) activate the crystallized subunits and stabilize the so obtained conformations. Although neither of these approaches is simple or routine, we exploited them for the determination of high-resolution functionally relevant structures.

Conformational Mobility of the Small Ribosomal Subunit

The small subunit is built of loosely attached domains (Figure 2) and contains structural elements that allow local rearrangements as well as the global motions required for its function. Its conformational variability has been detected by cryo electron microscopy (Gabashvili *et al*., 2001, Stark *et al*., 1997), by surface RNA probing (Alexander *et al*., 1994), by monitoring ribosomal activity, and by the analysis of the high resolution structures of the small subunit complexes (Carter *et al*., 2000, Schluenzen *et al*., 2000, Wimberly *et al*., 2000, Pioletti *et al*., 2001, Clemons *et al*., 2001, Ogle *et al*., 2001). The conformational variability also explains why all the available cryo-EM reconstructions were not useful for extracting initial phase sets for the small subunit, whereas similar searches were performed successfully for the whole ribosome and for its large ribosomal subunit (Harms *et al*., 1999). Our analysis of the 30S structure led us to suggest an interconnected network of features that could allow concerted movements during translocation. This movement includes the formation of a pore of varying diameter between the head and the shoulder, and is associated with the concerted displacement of the platform facilitate mRNA threading and progression and provides the special geometry that guarantees processivity of and ensures maximized fidelity of the biosynthetic process.

The head makes the upper boundary of the mRNA channel, and its relative location is dictated by the head twist. In addition, internal head axes may be utilized for facilitating global movements associated with protein biosynthesis. Head mobility was confirmed by molecular replacement studies that indicated that the low-resolution crystals contain at least one conformation that differs from that of the crystals diffracting to high resolution. The pivotal point for this movement is likely to be at the connection between the head and the neck, rather close to the binding site of the antibiotic spectinomycin that is known to hamper the head twist by trapping a particular conformation (Carter *et al*., 2000).

Trapping crystalline small subunit at functionally relevant conformations

The small ribosomal subunit is less stable than the large one. We found that by exposing 70S ribosomes to a potent proteolytic mixture, the 50S subunits remained intact, whereas the 30S subunits were completely digested (Evers *et al*., 1994). Similarly, large differences in the integrity of the two subunits were observed when attempting crystallization of entire ribosomes assembled from purified subunits. Crystals obtained from these preparations were found to consist only of 50S subunits (Berkovitch-Yellin *et al*., 1992) and the supernatant of the crystallization drop did not contain intact small subunits, but did show 30S proteins and fragmented 16S RNA chain. Consequently, among the many ribosome sources that were tested, so far only the 30S from *T. thermophilus* crystallized, and only one crystal-type of the small subunit was found suitable for crystallographic studies. Almost a decade was needed to minimize the severe non-isomorphism of this form and all the procedures developed for increasing the homogeneity of these crystals, are based on post-crystallization treatments.

Our approach (Tocilj *et al*., 1999, Schluenzen *et al*., 2000) was to induce a preferred conformation within the crystals, preferably, a conformation with functional relevance. We exploited the commonly used heat-activation procedure, developed over 30 years ago (Zamir *et al*., 1971). We exposed the T30S crystals to elevated temperatures, since we suspected that their specific packing arrangement should allow post-

crystallization conformational rearrangements. As the first task of the small ribosomal subunit is to form the initiation complex, we assumed that the heat induced conformation resembles this one. Once functional activation was achieved, the conformation of the particles was stabilized by incubation the crystals with minute amounts of a heteropolytungstate cluster [$(NH_4)_6(P_2W_{18}O_{62})14H_2O$], referred below as W18 (Tocilj *et al*., 1999). The same procedure was employed for complexes of T30S with compounds that facilitate or inhibit protein biosynthesis, mRNA analogues, initiation factors and antibiotics. Soaking in solutions containing the non-ribosomal compounds in their normal binding buffer was performed at elevated temperatures. Once the functional complex was formed, the crystals were treated with W18 cluster.

We found in the low resolution crystals of T30S various head conformations (Figure 2), including the conformation seen at high resolution. Head stability was achieved by the interactions of four W18 clusters with protein S2 (Figure 2), a large and flexible ribosomal protein, located on the solvent side of the 30S particle and combining the head to the body. Since S2 is located on a crystallographic two-fold axis, the W18 clusters "glued" the symmetry related two particles, hindered the movements of protein S2, and consequently also of the entire head. A similar effect was obtained by binding spectinomycin, an antibiotic agent that locks the head of the small subunit in a particular conformation, and was reported to improve the quality of the T30S crystals (Carter *et al*., 2000). Thus, although the mechanism for minimizing internal motions differs in the two systems, and although only in one system effort was made to achieve a functionally relevant conformation (Tocilj *et al*., 1999, Schluenzen *et al*., 2001), the resulting fixation of the desired conformation led to better diffracting crystals.

The W18 cluster played a dual role in the course of structure determination of T30S. In additions to minimizing the conformational heterogeneity and limiting the mobility of the crystallized particles, treatment with this cluster yielded phase information. Thirteen W18 clusters bind to each T30S particle. The individual W atoms of ten of them (total 180 atoms) could be located precisely. Most of tungsten clusters interact with ribosomal proteins (Figure 2), in positions that may significantly reduce the global mobility of the T30S particles within the crystal network.

Pairing of T30S particles around the crystallographic two-fold axis is one of the main features of the crystallographic network in T30S crystals. The contacts holding these pairs are extremely stable, and many of them were maintained even after the rest of the crystal network is destroyed (Harms *et al*., 1999).

Edeine — A universal antibiotic limiting platform mobility

The small subunit is the main player in initiation of protein biosynthesis. After binding to the mRNA the initiation complex moves in the 5' to 3' direction along the mRNA scanning it, in search for the initiator (AUG) codon (Kozak and Shatkin, 1978). Edeine is a peptide-like antibiotic agent, produced by a strain of *Bacillus brevis*. It contains a spermidine-type moiety at its C-terminal end and a beta-tyrosine residue at its N-terminal end (Kurylo-Borowska, 1975). As early as 1976 (Fresno *et al*., 1976) it was found that the universal antibiotic edeine blocks mRNA binding to the small ribosomal subunit. Further biochemical studies indicated that edeine inhibits mRNA binding by linking critical features translocation and E-site tRNA release, and impose constraints on ribosomal mobility required for the translation process (Altamura *et al*., 1988, Odom *et al*., 1978).

We found that it binds to the platform in a position that may affect the binding of the P-site tRNA, alter the mRNA path at the E-site and hamper the interactions between the small and the large subunits (Pioletti *et al*., 2001). This is consistent with the finding that a subset of the 16S rRNA nucleotides protected by the P-site tRNA (Moazed *et al*., 1995) overlaps with those protected by edeine, kasugamycin and pactamycin (Mankin, 1997, Woodcock *et al*., 1991). In addition, the binding of edeine to the 30S subunit induces the formation of a new base pair (Figure 2) that may alter the mRNA path and would impose constraints on the mobility of the platform. Thus, by physically linking the mRNA and four key helices that are critical for tRNA and mRNA binding, edeine locks the small subunit into a fixed configuration and hinder the conformational changes that accompany the initiation process.

The universal effect of edeine on initiation implies that the main structural elements important for the initiation process are conserved in

all kingdoms. Analysis of our results shows that all rRNA bases defining the edeine-binding site are conserved in chloroplasts, mitochondria, and the three phylogenetic domains. Among these are two conserved nucleotides along the path of the messenger. Thus, edeine shows a novel mode of action, based on limiting the ribosomal mobility and/or preventing the ribosome from adopting conformations required for its function. Furthermore, it induces an allosteric change by the formation of a new base pair–an important new principle of antibiotic action.

CONFORMATIONAL MOBILITY WITHIN THE LARGE RIBOSOMAL SUBUNIT

The structure of the large ribosomal subunit was reported to be compact and monolithic (Ban *et al*., 2000). Nevertheless, significant mobility was assigned to the large subunit's features that are directly involved in ribosomal functions, based on cryo electron microscopy studies (Frank and Agrawal, 2000), as well as on comparisons of the crystal structures of the entire ribosome with the structures of its large ribosomal subunit. The latter showed that most of the functionally relevant features of the large subunit assume different conformations in unbound (Harms *et al*., 2001, Yonath, 2002) and assembled (Yusupov *et al*., 2001) states. They also may become completely disordered, as in the 2.4 Å crystal structure of the large subunits from *Haloarcula marismortui,* H50S (Ban *et al*., 2000).

The conformational variability of the large subunit allows the creation of intersubunit bridges, leads to the formation of peptide bonds, facilitates tRNA release, and enables the involvement of the ribosome in cell regulation. The flexibility of the functionally relevant features is manifested in the variability of their conformations between the unbound D50S subunits, and those incorporated into T70S ribosomes, as well as in their disorder in H50S. Thus, almost all of the RNA structural features known to be involved in functional aspects of protein biosynthesis are disordered in the 2.4 Å electron density map of H50S (Ban *et al*., 2000). These include both lateral protuberances that create the most prominent features in the typical shape of the large subunit; intersubunit bridges and four ribosomal proteins, all of them match the list of proteins that are

loosely held by the core of the particle, hence could be detached selectively from halophilic ribosomes (Franceschi *et al*., 1994).

A revolving door assisting the release of E-site tRNA

Although the large ribosomal subunit is known to have less conformational variability than the small subunit, it does posses various conformations that can be correlated to the functional activity of the ribosome. The most significant differences between the two structures of the unbound large subunits were found in key features, known to participate in the functional activities of the ribosome. Remarkable examples are the 50S hook into the decoding region of the small subunit, and other intersubunit bridges created upon subunit association, the entire L1 arm that acts as the revolving gate for the exiting tRNA molecules, and the GTPase center.

The L1 stalk, which includes the rRNA helices and a ribosomal protein, L1, is well resolved in T70S (Yusupov *et al*., 2001) and in D50S (Harms *et al*., 2001). Comparison between the structure of the unbound 50S and the 70S ribosome indicates how the L1-arm facilitates the exit of the tRNA molecules. In the complex of T70S with three tRNA molecules, the L1 stalk interacts with the elbow of E-tRNA. This interaction seems to block the release of the E-site tRNA. In H50S, the entire L1 arm is disordered and therefore could not be traced in the electron density map (Ban *et al*., 2000), an additional hint of the inherent flexibility of this feature.

The location of protein L1 in D50S does not block the presumed exit path of the E-site tRNA, hence it seems that the mobility of the L1 arm is utilized for facilitating the release of E-site tRNA. Although the orientation of the L1 arm in the 70S ribosome during the release of the E-site tRNA is still not known, the two defined orientations that have been observed indicated that movement of the L1 arm might occur during protein biosynthesis. Superposition of the structure of D50S on that of the T70S ribosome allowed the definition of a pivot point for the possible movement of the L1 arm. Similar differences found in the relative orientation of the L1 stalk have been correlated with the presence or absence of tRNA and elongation factors (Agrawal *et al*., 2000). Hence it may be assumed that the position of the L1 stalk in the unbound D50S represents the conformational change required for the release of the E-site tRNA.

An intersubunit bridge with multiple roles

Intersubunit bridges form upon the association of the two ribosomal subunits, once the functionally active is created. They are the features connecting the two subunits within the assembled ribosome, namely the linkers between the two ribosomal subunits. The correct assembly of the entire ribosome from its two subunits is the key, or one of the major keys, for proteins biosynthesis, hence these bridges must be positioned accurately and point at the exact direction. Each intersubunit bridge is formed from two parts – one of the small and one of the large subunit. We found that whereas those of the small subunit are of almost the same conformation in the unbound and bound subunit, those originating from the large one are inherently flexible, and may have different conformations or assume a high level of disorder. Upon subunit association the conformations of these bridges change so that they can participate in the creation of the assembled ribosome. Thus, their structure and the nature of their conformational mobility should show how the ribosome controls its intricate assembly.

Fig. 3. (Figure on facing page)
(a) The RNA domains of D50S (color code is shown in the middle). Top: Left – front (interface) view. Right: solvent side. Bottom: side views, obtained by rotating the top views around their long axis by 90 degrees. The interface views are flat, with perturbing L1 stalk (in yellow).
(b) The upper part of D50S (compared to the view shown in the a top left). The L1-arm of D50S is highlighted (in gold). Also shown are the docked L1-arm of T70S and protein L1 of T70S (green) and the location of protein L1 in D50S (yellow-gold). The pivot point between these two orientations is marked by a red dot. The docked tRNA molecules are shown in cyan (A), blue (P) and purple (E).
(c) Bridge B2a (H69) in the unbound D50S (red) and within the T70S ribosome (gold). H44 (of the small subunit) is shown in gray. P-site tRNA (in cyan) and A-site in green.
(d) The modified bases in the tip of H69 are shown.
(e) and (f) show overlay of H69 In the unbound D50S subunit (gray) on the corresponding feature in the structure of the whole ribosome (gold). The tRNA acceptor stem mimic (ASM) is shown in red. The docked A- and P-sites tRNA are shown in cyan and dark green (respectively). These figures indicate the proposed movement of H69 towards the decoding center of H44 (light cyan) in T30S.

These bridges could be seen even at 5.5 Å resolution, and are described in detail in (Yusupov *et al*., 2001). Here we focus on bridge B2a for a few functional tasks, since we found that elements involved in bridging the two subunits within the assembled ribosome, appear to participate in the functional tasks of the ribosome. The orientation of H69 with its universally conserved stem-loop in D50S is different than that seen in T70S. Both lie on the surface of the intersubunit interface, but in the 70S ribosome it stretches towards the small subunit, whereas in the

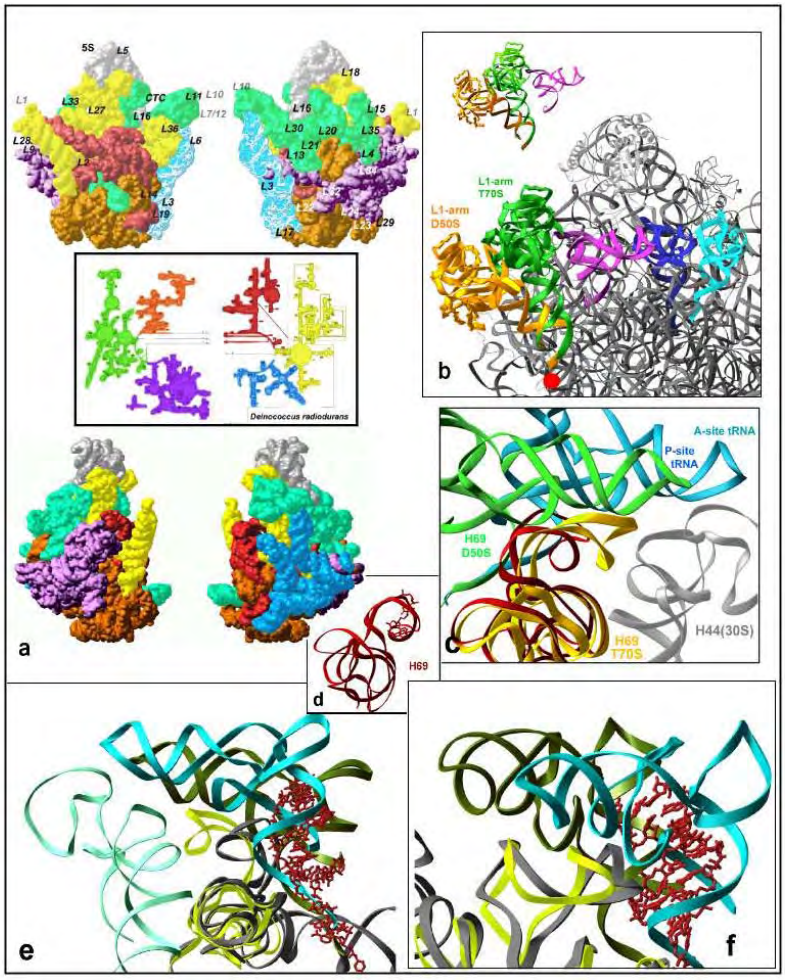

Fig. 3.

free 50S it makes more contacts with the large subunit, so that the distance between the tips of their stem-loops is about 13.5 Å. Figure 3c hints at a feasible sequence of events leading to its creation. Once the initiation complex, that includes the small subunit and tRNA at the P-site, approaches the large subunit the tRNA pushes helix H69 towards the decoding center, and the intersubunit bridge is formed.

The specific conformations of H69 in D50S and T50S, and their modes of binding the tRNA and its mimics, implicated H69 as a carrier of the helical part of the A-site tRNA into the P-site. Within the 70S ribosome, H69 interacts with both the A- and the P-site tRNAs (Yusupov *et al*., 2001). In the complex of D50S with an acceptor stem tRNA mimic (called here ASM), most of the contacts of the helical stem of the ASM, which position it within the A-site, are with H69 (Figure 4). The crucial contribution of H69 to the proper placement of the tRNA mimic is also reflected by the disorder of the helical stem of the tRNA mimic that was bound to H50S crystals, in which H69 itself is disordered (Ban *et al*., 2000, Nissen *et al*., 2000).

The displacement and the rotation of a massive helix like H69 require inherent flexibility. It is conceivable that the ribosome benefits from this flexibility beyond bridging the two subunits. The proximity of H69 to both the A- and the P-site tRNAs (Yusupov *et al*., 2001, Bashan *et al*., 2002), suggest that besides acting as an intersubunit bridge, H69 participates in translocation. In addition, connecting between the peptidyl transferase center in the large subunit and the decoding region (Figure 3) in the small one, H69 may be the right candidate to provide the machinery needed for the transmission of signals between the two centers. The location of H69 may hint also at its contribution to a sophisticated signaling network over long distances, like between the GTPase and the PTC centers or between the PTC and the E-site tRNA release mechanism (Harms *et al*., 2001).

Interestingly, mapping of the *E. coli* modified nucleotides known to be important for the function of the large ribosomal subunit (Ofengand and Bakin, 1997) onto the D50S structure, showed clustering of the positions corresponding to these nucleotides in the vicinity of the active site of *D. radiodurans* as well as in H69 (Figures 3 and 5). The location of the latter on the stem loop of H69 intersubunit bridge in the assembled

ribosome led us to suggest that the modified bases play a role in the bridging events.

The PTC tolerates various binding modes

Three-dimensional structures of several complexes of D50S with substrate analogs, designed to mimic the tRNA acceptor stem (ASM) or the CCA 3' end of the tRNA bound to puromycin (ACCP), with the universal antibiotic sparsomycin, and with a combination of ASM and sparsomycin (ASMS) were determined by us (Bashan *et al*., 2002). Analysis of these structures allowed us to elucidate the modes of interactions between the ribosome and the substrate analogs; to illuminate elements of flexibility within the peptidyl transferase cavity, including those facilitating the interplay between the A- and P-sites; to investigate the principles of the action of a P-site ligand; and to identify feature that contribute to the dynamics of translocation.

The PTC is highly conserved. Nevertheless, we observed some diversity in its structure in the different crystal systems. The overall structure of the cavity hosting the PT activity in the liganded D50S is similar to that seen in the native (Harms *et al*., 2001), in the antibiotic bound D50S structures (Schluenzen *et al*., 2001) and in the complexed 70S ribosome (Yusupov *et al*., 2001). The orientations of both the conserved and variable bases of the PTC seem to depend on several parameters; among them is the functional state of the ribosome. Thus, the conformation of the key nucleotides in the complex of T70S with three tRNAs differs significantly from the conformations seen in two complexes of the large ribosomal subunit from H50S with compounds believed to be substrate or transition-state analogs (Yusupov *et al*., 2001). Also, the PTC of H50S undergoes notable conformational changes upon binding ligands (Nissen *et al*., 2000, Schmeing *et al*., 2002), including the ordering of the base corresponding to A2602, which is disordered in the 2.4 Å structure of H50S, as are most of the functionally relevant features in this structure (Ban *et al*., 2000).

Diversity in binding modes of different A-site tRNA analogs may also be connected to the nature of the analog, and the differences in positioning of different analogs appear to be correlated with the amount of

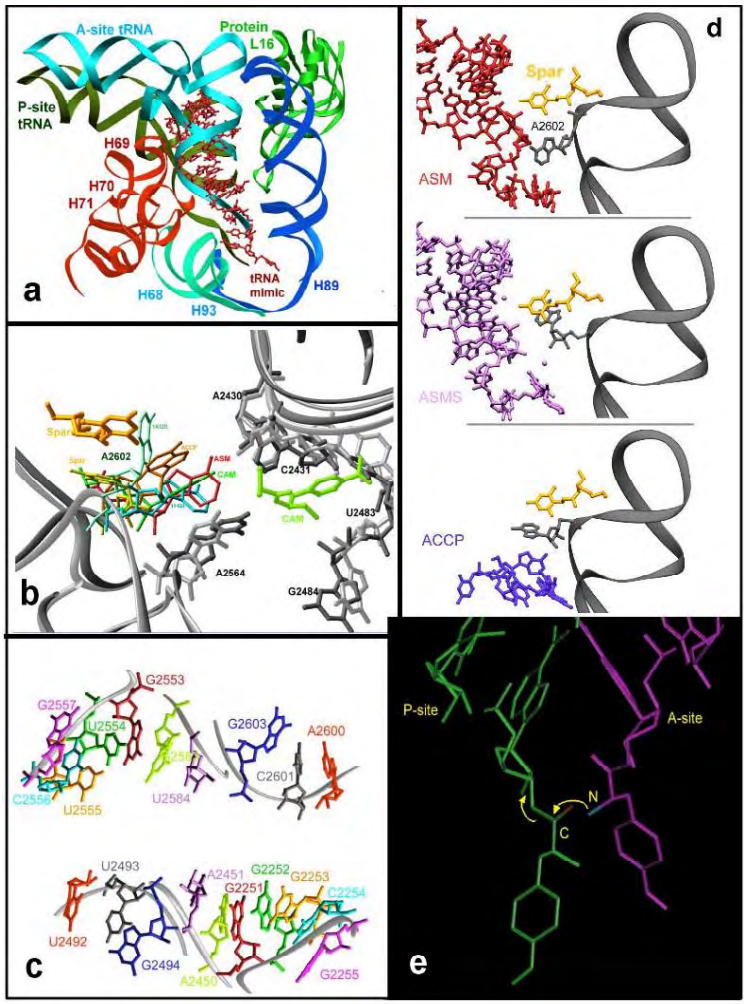

Fig. 4 (a) The PTC and its environment, including ASM and the modeled A- and P-site tRNAs.
(b) Three views, showing substrate analogs in the PTC and, backbone of H93 and A2602. Note the hydrated Mg^{2+} ions, shown as pink dots.
(c) The relative orientations of A2602 in different complexes of D50S (Bashan *et al.*, 2002) and of H50S (PDB entry 1FGO and 1KQS). Sparsomycin (Spar) and chloramphenicol (CAM) are included, to indicate the limits of the rotation ofA2602. The dark gray indicates the RNA backbone in the sparsomycin/D50S complex. The light gray shows the backbone in D50S/CAM complex.
(d) The two fold symmetry in the PTC, together with A2602.
(e) The proposed over-all mechanism of peptide bond formation.

support given to them by the PTC. An example is ASM that is held in its position mostly by the interactions that its helical part makes with H69, the loop between H69 and H71 and protein L16 (Figure 4). The tRNA mimics that include features representing the acceptor stem of tRNA, were found to be oriented by their interactions with two long ribosomal helical segments, H89 and H69. Such contacts cannot be created either for short analogs or when one of the main supports, helix H69, is disordered, as in the structure of H50S. Indeed, we found that truncated substrate-analogs bind to the ribosomal peptidyl center at a large range of conformations that may be similar, but not identical, to the mode of binding of larger RNA constructs that were designed to bind to the large subunit as tRNA mimics.

We found that the compounds mimicking the CCA ends of tRNA, complexed with D50S (Bashan *et al*., 2002) or H50S (Nissen *et al*., 2000, Schmeing *et al*., 2002), are held in their positions by a comparable amount of interactions with their corresponding PTCs. However, variations in binding modes were observed between them, even within the subgroup of short tRNA analogs (Figure 4). Thus, it appears that the lower part of the PTC can tolerate several binding modes that resemble each other, but are not necessarily identical to the precise orientation leading to efficient protein biosynthesis. Consistent with the findings that although most of the interactions of the ACCP with the ribosome are with universally conserved nucleotides, altered reactivities were observed for puromycin in eubacteria and archaea (Rodriguez-Fonseca *et al*., 1995). The position of ASM in D50S is similar, but not identical, to that of the acceptor stem of the A-site tRNA in the 5.5 Å structure of T70S (Yusupov *et al*., 2001). The reasons for this may reflect the difference between tRNA binding to unbound large subunit and to assembled ribosome, in which the tRNA also makes substantial contacts with the small subunit, or to the differences in A-site binding in the absence of P-site substrate (Green *et al*., 1998). Alternatively, the position of ASM may indicate the existence of an additional binding mode, similar to the suggested "hybrid mode", in which the movement of the acceptor stem is uncoupled from that of the rest of the tRNA (Moazed and Noller, 1991).

The walls of the PT cavity are composed of several RNA features. One of them is the flexible helix H69 that forms the B2a bridge (Harms

et al., 2001, Yusupov *et al*., 2001). The helical stem of ASM interacts with the extended loop of protein L16, and that H69 packs groove-to-backbone with it. Hence it seems that H69 and protein L16 are the key factors influencing the positioning of ASM within the PTC. Interestingly, the main chain of protein does not interact directly with the tRNA mimic, although its conformation underwent substantial rearrangements as a result of the binding of the tRNA mimic, presumably to avoid short contacts.

Analysis of the modes of attachment of the tRNA mimics to the peptidyl transferase center in D50S supports the idea that the ribosome provides a frame for the peptide bond formation, rather than being actively involved in the catalytic events, consistent with (Polacek *et al*., 2001), and with the suggestion that di-metal ions may be instrumental for peptide bond formation (Barta *et al*., 2001). Our studies also indicate that the peptidyl transferase center contains several flexible regions, some of which may be stabilized by the binding of substrate analogs, others may be exploited as parts of the for translocation machinery.

Striking conformational alterations within the PTC

Sparsomycin is a universal antibiotic agent. Nevertheless, ribosomes from different kingdoms show differences in binding affinities to it. Similar to PTC antibiotics studied so far by us (Schluenzen *et al*., 2001), sparsomycin interacts exclusively of 23S RNA. In its single binding site, and interacts with the highly conserved base A2602. But, unlike other antibiotics of the large subunit, which make various interactions with the ribosome, sparsomycin interacts only with a single base, A2602. The limited contacts between sparsomycin and the large subunit rationalize its weak binding. These stacking interactions may be sufficient for its firm attachment as long as the ribosome or its large subunit are not actively involved in protein biosynthesis, or in the crystals, owing to the limited mobility of crystalline materials. In active ribosome, destabilization of sparsomycin binding during protein biosynthesis may be correlated to changes in the orientation of sparsomycin's counterpart, nucleotide A2602, which was implicated to play an active role in protein biosynthesis. Additional interactions with P-site substrates like N-blocked

aminoacyl-tRNA that is known to increase the accessibility of nucleotide A2602 (Porse *et al*., 1999), should lead to tighter binding. Furthermore, the enhancement of sparsomycin binding by N-blocked aminoacyl-tRNA may indicate that sparsomycin may inhibit protein biosynthesis not only by altering the conformation of the PTC, but also by blocking the P-site and by trapping non-productive intermediate-state compounds.

In contrast to the minor conformational changes induced by the antibiotics studied so far (Schluenzen *et al*., 2001), sparsomycin appears to significantly alter the conformation of both the P- and the A-sites. A2602 is the base that undergoes the most noticeable conformational rearrangements (Figure 4) upon sparsomycin binding. Interestingly, although chloramphenicol and sparsomycin do not share overlapping positions, they seem to compete with each other in inhibiting peptide bond formation. We found that the base of A2602 in sparsomycin complex is flipped by 180° compared with its position in the complex of D50S with chloramphenicol (Figure 4), implicating this base as the trigger of the competition between them.

Analysis of our results showed that sparsomycin introduces alterations in the peptidyl transferase center. Figure 3 shows the location of the tRNA mimic in the presence of sparsomycin. Compared with its position in "empty" PTC, in the presence of sparsomycin, ASM is slightly twisted and placed somewhat closer to the P-site. In its position ASMS interacts with protein L16, but looses one of the contacts that ASM makes with this protein. In addition to the interactions of ASMS with the 23S RNA and protein L16, it makes three hydrogen bonds with a putative hydrated Mg^{2+} ion, located close to its CCA end. This Mg^{2+} ion with the water molecules bound to it, is seen clearly in the ASMS map. The same position in the ASM map contains less well-defined features.

We assume that the differences between the binding modes of ASM and ASMS result from alterations in the PTC. Since ASMS crystals were obtained by soaking co-crystals of D50S and sparsomycin, and since sparsomycin was shown to trigger conformation changes n the PTC, it seems that these were sufficient to modify the binding mode of the A-site substrate analogs, hence suggesting interplay between the A- and the P-sites. Based on the binding modes of ASM in the presence and absence

of sparsomycin, we conclude that P-site occupation governs the positioning at the A-site. As seen below, whereas the location and orientation of the A-site acceptor stem analog (ASM) seems to be designed for peptide bond formation, the orientation of ASM in the presence of an inhibitor at the P-site, would not permit its participation in peptide bond formation. Thus, the PTC seems to possess a mechanism that prevents correct localization of a tRNA molecule at the A-site when the P-site is occupied by an inhibitor rather than a substrate.

Two-fold rotation

We identified a local two-fold rotation axis within the peptidyl transferase cavity that relates two groups of nine nucleotides, in each the A- and P-sites (Figure 4). Conformation, rather than the type of the base, is related by the pseudo two-fold symmetry. This local two-fold symmetry at the PTC of D50S is consistent with the observation that the CCAs bound in the A-and P-sites are related by a two-fold axis (Nissen *et al*., 2000).

Why does the structure of the ribosome, which lacks any symmetry, possess a local two-fold axis at its active site? Why are the 3'-ends of the A- and P-sites tRNAs related by a local two-fold axis, whereas the tRNAs molecules are related by translation? A feasible explanation is that the local two-fold symmetry provides similar, albeit not identical, environments for the CCA termini, to allow for a smooth translocation with minor rearrangements (Yusupov *et al*., 2001) and without being exposed to large energetical differences.

Translocation of the tRNA–mRNA complex involves disruption of existing interactions in one site and the establishment of new interactions in the next site. Owing to the local two-fold symmetry, the environments of the A- and P-sites are similar. Nevertheless, the environment of the 3' ends of the two tRNAs are somewhat different. In T70S crystals, the P-site tRNA seems to make more interactions with the P-loop than the A-site with the A-loop (Yusupov *et al*., 2001). In the liganded H50S crystals, the A- and the P-site tRNA make the same number of contacts with the PTC, but the P-site tRNA makes two base pairs whereas the A-site tRNA is involved in only one base pair[Nissen, 2000 #57. Hence, in both

systems the progression from the A- to the P-site would be energetically favored and should enhance the contacts between the tRNA and the 23S RNA.

The observation of a two fold symmetry between the A- and P-sites 3' tRNA termini implies that regardless of the translocation mechanism, the CCA end of the A-site tRNA bearing the newly formed polypeptide should rotate by approximately 180° on its way from the A- to the P-site. This rotation may be triggered by the creation of the new peptide bond, and can occur, in principle, when the helical part of the tRNA is either at the A-site, or during its translocation to the P-site or after the tRNA reaches the P-site. In order to exclude non-permitted rotations due to space constrains, we modeled the three possibilities for rotation (Agmon *et al*., to be published). Starting from the location of the tRNA mimic (ASM) in D50S, we found that a 180° rotation of its ACCA end together with the base bound to it can occur while the helical part of ASM is at the A-site without steric hindrance. Furthermore, we found that in ASM, the P-O3' bond corresponding to the bond connecting bases 73 and 74 of tRNA, are located just above the ACCA terminal, is almost overlapping the local two-fold axis. Therefore the ACCA-peptidyl rotation may occur around this bond while the tRNA is at a location similar to that of ASM that may represent an intermediate hybrid state (Moazed and Noller, 1989).

Performing the two-fold symmetry operation on ASM positioned the carbonyl carbon of esterified P site residue in an orientation and distance suitable for a nucleophilic attack of the primary amine of the A-site bound aminoacyl tRNA. At these relative orientations a nucleophilic attack should be spontaneous, especially at basic pH values, as in D50S, since the primary amine is not expected to be protonated. At this orientation similar mechanism should be possible even at slightly acidic pH values, ~6, as an equilibrium between NH2 and $NH3^+$ is expected. The optimal overall pH value for efficient protein biosynthesis of D50S (similar to many other ribosomes) is around pH=8. Hence, it is logical to expect that the pH of the local environment at the PTC should be between these two values. We therefore propose a mechanism for peptide-bond formation, which is based on direct donor-acceptor interaction

between the A- and P-substrates, and on proton transfer mediated by water or hydrated magnesium that was identified in the vicinity of the two substrates (Bashan *et al*., 2002). This mechanism is consistent with our earlier observations (Schluenzen *et al*., 2001, Yonath, 2002) as well as with earlier suggestions saying that the ribosome provides the frame for accurate orientation of the tRNA molecules and may enhances the rate of peptide bond formation (Nierhaus *et al*., 1980, Samaha *et al*., 1995, Green and Noller, 1997, Pape *et al*., 1999, Polacek *et al*., 2001) rather than participating in the actual enzymatic activity, as suggested by the Yale group (Nissen *et al*., 2000).

Nucleotides U2585 and A2602 are located approximately on the local two-fold axis, and U2585 is situated right under A2602, in the direction of the protein exit tunnel. This construction hints that the extremely flexible nucleotide A2602 may play a dynamic role in coordinating the tRNA motions, and U2585 may assist in guiding the ACCA during the rotation and in transmitting messages from the tunnel wall to the PTC. This suggested rotation-translation motion could provide benefits not only for translocation but also for the progression of the nascent protein through the tunnel, since it may create a screw motion that demands less force than straight pushing. As the walls of the exit tunnel have bumps and grooves and its diameter is not uniform, the progression of the nascent protein through the tunnel cannot be approximated to a smooth object progressing along smooth walls. The growing proteins move at times through narrow paths, so that their side chains may exercise significant friction. One of the narrowest regions of the tunnel is its entrance. Hence, a screw movement should be beneficial especially for the first step of nascent chain movement – its entry into the tunnel.

THE PROTEIN EXIT TUNNEL – A PASSIVE PATH OR AN ACTIVE DISCRIMINATOR?

The protein exit tunnel was assumed to provide a passive path for exporting smoothly all protein sequences and changes in its diameter were observed in correlation with mutations or different functional states (Gabashvili *et al*., 2001). Originally this tunnel was believed to provide a passive path to the nascent protein chains. However, evidence was

obtained for tunnel participation in regulating intracellular co-translational processes, indicated that the tunnel may possess dynamic capabilities allowing it to function as a discriminating gate and to respond to signals from cellular factors or from nascent proteins and references therein. Sequences that presumably interact with the tunnel interior and thereby arrest protein elongation cycle were identified. This interactive elongation arrest was proposed to provide mechanisms to guarantee critical events, such as sub-cellular localizations or subunit assembly (Walter and Johnson, 1994, Nakatogawa and Ito, 2002, Tenson and Ehrenberg, 2002, Young and Andrews, 1996, Stroud and Walter, 1999, Liao *et al*., 1997, Sarker *et al*., 2000). Furthermore, recently it was found that short peptides can act as regulatory nascent peptides and render resistance to macrolides (Herr *et al*., 2000, Lovett and Rogers, 1996, Tenson and Mankin, 2001, Weisblum, 1995), while exploiting the peptides translated by the same ribosome. The length and the sequence of the peptides are critical for their activity, suggesting direct interaction between the peptide and the drug on the ribosome.

GATING WITHIN THE TUNNEL: A MECHANISM FOR REGULATING SELECTED CELLULAR EVENTS

A semi-synthetic macrolide of no clinical use was found to trigger a striking conformational rearrangement in the walls of the tunnel, by flipping the tip of a highly conserved beta-hairpin of the ribosomal protein L22 across the tunnel (Figure 5). This modulation of the tunnel shape provides the first structural insight into its dynamics. The tunnel gating could be correlated with sequence discrimination and elongation arrest of the SecM (secretion monitor) protein (Sarker *et al*., 2000), thus paving the way for illuminating the ribosome role in regulating intracellular events. This secretory protein monitors protein export. It includes a sequence motif that causes arrest during translation in the absence of the protein export system (called also "pulling protein"), which can be bypassed by mutations in the ribosomal RNA (rRNA) or in ribosomal protein L22 (Nakatogawa and Ito, 2002), a constituent of the tunnel walls

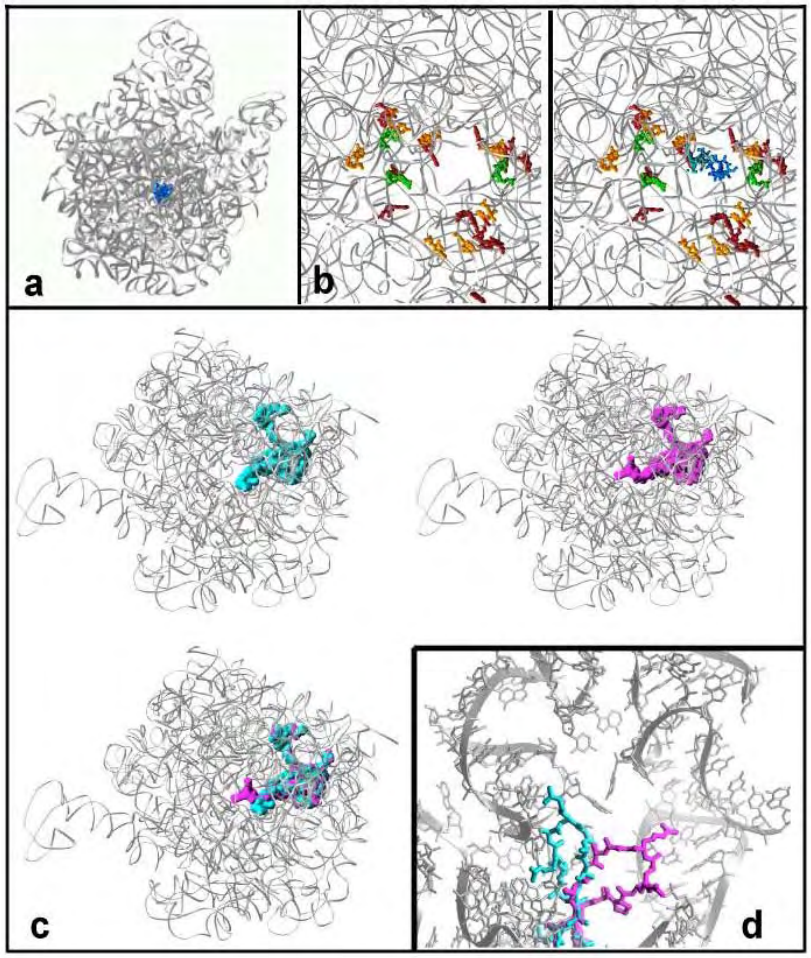

Fig. 5 (a) The interface view of D50S (only RNA backbone is shown). The position of the tunnel entrance is highlighted in blue (representing erythromycin at its binding site).
(b) Left: A view into the ribosomal exit tunnel highlighting all modified nucleotides (yellow: pseudouridines, red: methylations, green: sugars. Right: the same as in the left side, but with erythromycin in the tunnel.
(c) View into the ribosomal tunnel from the active site, showing the hindrance of the tunnel by L22 swung conformation (magenta, right) compared to the native (cyan, left). A superposition of them is shown in the bottom. Note how the native and swung double-hooks interact with two sides of the tunnel wall.
(d) Side view of the region of the ribosome exit tunnel, showing the contacts of the native (cyan) and swung (magenta) conformations of L22 hairpin tip. The RNA moieties constructing the tunnel wall at this region are shown in gray.

(Nissen *et al*., 2000, Harms *et al*., 2001). L22 consists of a single globular domain and a well-structured, highly conserved beta-hairpin with a unique twisted conformation, which maintains the same length in all species, whereas insertions/ deletions exist in other regions of L22. Within the ribosome protein L22 has an overall conformation similar to that seen in its crystal structure (Unge *et al*., 1998). Somewhat different, however, is the inclination of the tip of the beta-hairpin. It is positioned with its globular domain on the surface of the large subunit while the beta-hairpin lines the walls of the tunnel and extends approximately 30 Å away from the protein core.

Both the altered conformation of L22 beta-hairpin (called here the "swung conformation") and the native one are stabilized mainly by electrostatic interactions and hydrogen bonds with the backbone of rRNA. These two highly conserved arginines may be considered as a "double-hook" anchoring both native and swung conformations and modulating the switch between them. The structure of protein L22 appears to be designed for its gating role. Precise positioning of L22 hairpin stem, required for accurate swinging and anchoring of the double-hook is presumably achieved by the pronounced positive surface charges of this region.

The observation that sequence related translational arrest could be suppressed by mutations that were localized in the double-hook region of protein L22, led us to propose that the observed swing of the tip of L22 beta-hairpin indicate its intrinsic conformational mobility. Since the swung conformation restricts severely the space available for the passage of nascent proteins through the tunnel, and since L22 double-hook is highly conserved, it is logical to link the swing of L22 with the putative regulatory role assigned to the tunnel. We propose that L22 is a main player is this task, with its double-hook acting as a conformational switch and providing the molecular tool for the gating and discriminative properties of the ribosome tunnel.

A specific sequence motif that induces the elongation arrest while SecM protein is being formed was found to hinder translation elongation in *E. coli* even when present within unrelated sequences (Nakatogawa and Ito, 2002). We therefore suggest that the mechanism of the elongation arrest is based on the combination of the conformational rigidity of

protein with amino acids with bulky side chains (Trp and Ile) and their relative positions. By modeling a poly-alanine nascent chain, kinked to comply with the curvature of the tunnel, we verified that for this specific motif, once the proline has been incorporated into the nascent chain and was placed at the tunnel entrance, the two bulky amino acids reach the tip of L22 hairpin. In order to avoid collisions they may trigger a swing in a manner similar to ACM. This motion will free space for the bulky side chains, but at the same time will jam the tunnel for the progression of the nascent chain. In principle, nascent chains can use their flexibility to progress smoothly through the tunnel even in the proximity of L22 beta-hairpin, as presumably happens when residues with bulky sidechains are incorporated into nascent proteins. However, the inherent conformational rigidity of the proline that is located at the narrow entrance to the tunnel should hinder possible adjustments of the nascent chain.

Under normal conditions the SecM elongation arrest was found to be transient, but in the absence of active export of SecM the arrest is significantly prolonged (Nakatogawa and Ito, 2002). The question still to be investigated concerns the mechanism whereby the cellular signaling for alleviating the arrest is being transmitted. An intermediate conformation of the swung region may be required, allowing sufficient space for the bulky side chain and for progression of the nascent protein. Indications for such conformation were observed in the crystals structure of L22 (Unge *et al*., 1998). The conformational change of swung region may be triggered by the C-terminal end of L22, which is positioned at the vicinity of the exit tunnel opening (Nissen *et al*., 2000, Harms *et al*., 2001) and therefore may interact with the "pulling protein". This C-terminus of L22 is almost a linear extension of the beta-hairpin. Hence it may trigger allosteric rearrangements in the hairpin. The nascent chain may also play a role, since the arrest motif is located over 150 residues away from the N-terminal. Hence, once the bulky side chains reach the swung region of L22, the N-terminal residues of SecM should have reached the tunnel opening and can interact with the "pulling protein". The outstanding role of L22 and the conservation of the double hook, and of the hairpin size and sequence, suggest the gross discriminating mechanism to be universal, although the detailed interactions between the nascent protein and

the tunnel may vary between prokaryotes and higher organism. The known dependence of elongation arrest on sequence motifs within nascent peptides; the correlation between arrest-suppression mutants and the features involved in L22 gating induced by the modified macrolide; indicate that the tunnel is involved in sequence discrimination and may play active roles in regulation of intracellular processes.

Our results show that protein L22 has an intrinsic conformational mobility and contains a conserved double-hook feature, capable of interacting with the two sides of the tunnel wall, thus creating a swinging gate within the tunnel. The existence of dynamic features within the ribosomal tunnel and its ability to oscillate between conformations, the known dependence of elongation arrest on sequence motifs within nascent peptides, the correlation between arrest-suppression mutants and the features involved in L22 gating, indicate that the tunnel is involved in sequence discrimination and may play active roles in regulation of intracellular processes.

The opening of the ribosomal exit tunnel is located at the bottom of the particle. In D50S it is composed of rRNA components as well as of several proteins, including L22. In H50S, two proteins that do not exist in D50S, L31e L39e are also part of the lower part of the tunnel (Harms *et al*., 2001). Interestingly, the space occupied by protein L23 in D50S hosts two proteins in H50S, so that the halophilic L39e replaces the extended loop of L23 in D50S. L39e is a small protein of an extended nonglobular conformation, thinner than the extended loop of L23 in D50S. Therefore it penetrates deeper into the tunnel walls than the loop of L23 in D50S. L39e is present in archaea and eukaryotes, but not in eubacteria. Thus, it seems that with the increase in cellular complication, and perhaps as a consequence of the high salinity, a tighter control on the tunnel's exit was required, hence two proteins replace single one.

CONCLUDING REMARKS

Ribosomal crystallography, initiated two decades ago, yielded exciting structural and clinical information. We found that both the decoding center and the peptidyl transferase centers are formed of RNA. Proteins seem to serve ancillary functions such as stabilizing required conforma-

tion, binding of non-ribosomal factors, assisting the directionality of the translocation and gating of the ribosomal tunnel.

The ribosome is an accurate and intricate machine, and as such it has ample of mobile regions. These include the head and the shoulder of the small subunit, the features lining the mRNA path; the peptidyl transferase; the intersubunit bridges; the exit tunnel that control the release of nascent chains; the L1 stalk that provides the door for exiting tRNA.

The studies presented here show that the peptidyl transferase center tolerates various binding modes, but precise positioning appears to be crucial for the biosynthesis of protein chains. This precise positioning is determined by the tRNA helical stem, rather than by its 3' end, and the ribosome provides the structural frame for it. Once properly positioned, the peptide bond can be formed spontaneously. Ribosomal components appear not participate directly in the catalytic event. They may, however, be of major importance for cell vitality, as they may increase the efficiency or enhance the rate of the reaction..

Ribosomes are a major target for antibiotics. The therapeutic use of antibiotics has been severely hampered by the emergence of drug resistance in many pathogenic bacteria. With the increased popularity of antibiotics to treat bacterial infections, pathogenic strains have acquired antibiotic resistance, thus became ineffective. Resistance posed extremely serious medical problems that have prompted extensive effort in the design of modified or new antibacterial agents. The findings shown here may assist not only rational drug design but also open the door for minimizing drug resistance.

ACKNOWLEDGEMENTS

Thanks are due to J.M. Lehn, M. Lahav, A. Mankin and R. Wimmer for critical discussions, M. Pope for supplying us with tungsten clusters, M. Kessler for her superb assistance and to all the members ribosomal-crystallography groups at the Weizmann Institute and the Max-Planck Society for contributing to different stages of these studies. These studies could not be performed without the cooperation and assistance of the staff of station ID19 of the SBC at APS/ANL. The Max-Planck Society, the US National Institute of Health (GM34360), the German Ministry for

Science and Technology (BMBF Grant 05-641EA), and the Kimmelman Center for Macromolecular Assembly at the Weizmann Institute provided support. AY holds the Hellen and Martin Kimmel Professorial Chair.

REFERENCES

1. Agmon I. Auerbach T, Baram D, Bartels H, Bashan A, Berisio R, Fucini P, Hansen HAS, Harms J, Kessler M, Peretz M, Schluenzen F, Yonath A, Zarivach R. On peptide bond formation, translocation, nascent protein progression and the regulatory properties of ribosomes, *Eur J Biochem*, 2003; **270**: 2543.
2. Agrawal RK, Spahn CM, Penczek P, Grassucci RA, Nierhaus KH, Frank, J. Visualization of tRNA movements on the Escherichia coli 70S ribosome during the elongation cycle. *J Cell Biol*, 2000; **150**: 447–60.
3. Alexander RW, Muralikrishna P, Cooperman BS. Ribosomal Components Neighboring the Conserved 518-533-Loop of 16S Ribosomal-RNA in 30S Subunits. *Biochemistry*, 1994; **33**: 12109–18.
4. Altamura S, Sanz JL, Amils R, Cammarano P, Londei P. The Antibiotic Sensitivity Spectra of Ribosomes from the Thermoproteales Phylogenetic Depth and Distribution of Antibiotic Binding Sites. *Syst App Microbiol*, 1988; **10**: 218–25.
5. Ban N, Nissen P, Hansen J, Moore PB, Steitz TA. The complete atomic structure of the large ribosomal subunit at 2.4 A resolution. Science, 2000; **289**: 905–20.
6. Barta A, Dorner S, Polacek N. Mechanism of ribosomal peptide bond formation. Science, 2001; **291**: 203.
7. Bashan A, Agmon I, Zarivach R, Schluenzen F, Harms J, Berisio R, Bartels H, Franceschi F, Auerbach T, Hansen HAS, Kossoy E,Kessler M, Yonath A. Structural basis for a unified machinery of peptide bond formation, translocation and nascent chain progression. *Mol Cell,* 2003; **11**: 91.
8. Bayfield MA, Dahlberg AE, Schulmeister U, Dorner S, Barta A. A conformational change in the ribosomal peptidyl transferase center upon active/inactive transition. *Proc Natl Acad Sci* USA, 2001; **98**: 10096–101.
9. Berisio R, Schluenzen F, Harms J, Bashan A, Auerbach T, Baram D, Yonath A. Structural insight into the role of the ribosomal tunnel in cellular regulation. *Nat Struct Biol ,* 2003a;**10**: 366

10. Berisio R, Harms J, Schluenzen F, Zarivach R, Hansen HAS, Fucini P, Yonath A. Structural insight into the antibiotic action of telithromycin on resistant mutants. *J Bacteriol,* 2003b; **185**: 4276
11. Berkovitch-Yellin Z, Bennett WS, Yonath A. Aspects in structural studies on ribosomes. *Crit Rev Biochem Mol Biol*, 1992; **27**: 403–44.
12. Bourd SB, Kukhanova MK, Gottikh BP, Krayevsky AA. Cooperative effects in the peptidyltransferase center of Escherichia coli ribosomes. *Eur J Biochem*, 1983; **135**: 465–70.
13. Brodersen DE, Clemons WM Jr, Carter AP, Morgan-Warren RJ, Wimberly BT, Ramakrishnan V. The structural basis for the action of the antibiotics tetracycline, pactamycin, and hygromycin B on the 30S ribosomal subunit. *Cell*, 2000; **103**: 1143–54.
14. Carter AP, Clemons WM, Brodersen DE, Morgan-Warren RJ, Wimberly BT, Ramakrishnan V. Functional insights from the structure of the 30S ribosomal subunit and its interactions with antibiotics. *Nature*, 2000; **407**: 340–8.
15. Clemons WM Jr, Brodersen DE, McCutcheon JP, May JL, Carter AP, Morgan-Warren RJ, Wimberly BT, Ramakrishnan V. Crystal structure of the 30 S ribosomal subunit from Thermus thermophilus: purification, crystallization and structure determination. *J Mol Biol*, 2001; **310**: 827–43.
16. Cundliffe E. Antibiotic inhibitors of ribosome function, Wiley, London, New York, Sydney, Toronto, 1981.
17. Cundliffe E. In The Ribosome: structure, function and evolution, Eds Hill WE, Dahlberg AE, Garrett RA, Moore PB, Schlessinger D, Warner JR. ASM, Washington DC, 479–490, 1990.
18. Davydova N, Streltsov V, Wilce M, Liljas A, Garber M, L22 Ribosomal Protein and Effect of Its Mutation on Ribosome Resistance to Erythromycin, *J Mol Biol,* 2002;*322:*635
19. Ever SU, Franceschi F, Boddeker N, Yonath A. Crystallography of halophilic ribosome: the isolation of an internal ribonucleoprotein complex. *Biophys Chem*, 1994; **50**: 3–16.
20. Franceschi F, Sagi I, Boeddeker N, Evers U, Arndt E, Paulke C, Hasenban R, Laschever M, Glotz C, Piefke J, Muessi J, Weinstein S, Yonath A. Crystallography, biochemical and genetics studies on halophilic ribosomes. *Syst App Microbiol*, 1994; **16**: 697.
21. Frank J, Agrawal RK. A ratchet-like inter-subunit reorganization of the ribosome during translocation. *Nature*, 2000; **406**: 318–22.

22. Fresno M, Carrasco L, Vazquez D. Initiation of the polypeptide chain by reticulocyte cell-free systems. Survey of different inhibitors of translation. *Eur J Biochem*, 1976; **68**: 355–64.
23. Gabashvili IS, Gregory ST, Valle M, Grassucci R, Worbs M, Wahl MC, Dahlberg AE, Frank J. The polypeptide tunnel system in the ribosome and its gating in erythromycin resistance mutants of L4 and L22. *Mol Cell*, 2001; **8**: 181–8.
24. Gale EF, Cundliffe E, Reynolds PE, Richmond MH, Waring MJ. Wiley, London, 1981.
25. Garrett RA, Rodriguez-Fonseca C. In Ribosomal RNA: structure, evolution, processing & function, Eds, Zimmermann RA Dahlberg AE, CRC Press, Boca Raton, pp. 327–55, 1995.
26. Gluehmann M, Zarivach R, Bashan A, Harms J, Schluenzen F, Bartels H, Agmon I, Rosenblum G, Pioletti M, Auerbach T, Avila H, Hansen HA, Franceschi F, Yonath A. Ribosomal crystallography: from poorly diffracting microcrystals to high-resolution structures. *Methods*, 2001; **25**: 292–302.
27. Green R, Noller HF. Ribosomes and translation. *Annu Rev Biochem*, 1997; **66**: 679–716.
28. Green R, Switzer C, Noller HF. Ribosome-catalyzed peptide-bond formation with an A-site substrate covalently linked to 23S ribosomal RNA. *Science*, 1998; **280**: 286–9.
29. Hansen HA, Volkmann N, Piefke J, Glotz C, Weinstein S, Makowski I, Meyer S, Wittmann HG, Yonath A. Crystals of complexes mimicking protein biosynthesis are suitable for crystallographic studies. *Biochim Biophys Acta*, 1990; **1050**: 1–7.
30. Hansen JL, Schmeing TM, Moore PB, Steitz TA Structural insights into peptide bond formation, *Proc Natl Acad Sci USA*, 2002;***9****:*11670
31. Harms J, Schluenzen F, Zarivach R, Bashan A, Gat S, Agmon I, Bartels H, Franceschi F, Yonath A. High resolution structure of the large ribosomal subunit from a mesophilic eubacterium. *Cell*, 2001; **107**: 679–88.
32. Harms J, Tocilj A, Levin I, Agmon I, Stark H, Kolln I, van Heel M, Cuff M, Schlunzen F, Bashan A, Franceschi F, Yonath A. Elucidating the medium-resolution structure of ribosomal particles: an interplay between electron cryo-microscopy and X-ray crystallograhy. *Structure Fold Des*, 1999; **7**: 931–941.

33. Herr AJ, Gesteland RF, Atkins JF. One protein from two open reading frames: mechanism of a 50 nt translational bypass. *Embo J*, 2000; **19**: 2671–80.
34. Hope H, Frolow F, von Bohlen K, Makowski I, Kratky C, Halfon Y, Danz H, Webster P, Bartels KS, Wittmann HG, *et al*. Cryocrystallography of ribosomal particles. *Acta Crystallogr B*, 1989; **45**: 190–9.
35. Huang H, Chopra R, Verdine GL, Harrison, SC. Structure of a covalently trapped catalytic complex of HIV-1 reverse transcriptase: implications for drug resistance. *Science*, 1998; **282**: 1669–75.
36. Kirillov S, Porse BT, Vester B, Woolley P, Garrett RA. Movement of the 3'-end of tRNA through the peptidyl transferase centre and its inhibition by antibiotics. *FEBS Lett*, 1997; **406**: 223–33.
37. Kozak M, Shatkin AJ. Migration of 40 S ribosomal subunits on messenger RNA in the presence of edeine. *J Biol Chem*, 1978; **253**: 6568–77.
38. Kurylo-Borowska Z. Biosynthesis of edeine: II. Localization of edeine synthetase within Bacillus brevis Vm4. *Biochim Biophys Acta*, 1975; **399**: 31–41.
39. Lake JA. Evolving ribosome structure: domains in archaebacteria, eubacteria, eocytes and eukaryotes. *Annu Rev Biochem*, 1985; **54**: 507–30.
40. Liao S, Lin J, Do H, Johnson AE. Both lumenal and cytosolic gating of the aqueous ER translocon pore are regulated from inside the ribosome during membrane protein integration. *Cell*, 1997; **90**: 31–41.
41. Lill R, Wintermeyer W. Destabilization of codon-anticodon interaction in the ribosomal exit site. *J Mol Biol*, 1987; **196**: 137–48.
42. Lodmell JS, Dahlberg AE. A conformational switch in Escherichia coli 16S ribosomal RNA during decoding of messenger RNA. *Science*, 1997; **277**: 1262–7.
43. Lovett PS, Rogers EJ. Ribosome regulation by the nascent peptide. *Microbiol Rev*, 1996; **60**: 366–85.
44. Luger K, Mader AW, Richmond RK, Sargent DF, Richmond TJ. Crystal structure of the nucleosome core particle at 2.8 A resolution. *Nature*, 1997; **389**: 251–60.
45. Makowski I, Frolow F, Saper MA, Shoham M, Wittmann HG, Yonath A. Single crystals of large ribosomal particles from Halobacterium marismortui diffract to 6 A. *J Mol Biol*, 1987; **193**: 819–22.
46. Malkin LI, Rich A. Partial resistance of nascent polypeptide chains to proteolytic digestion due to ribosomal shielding. *J Mol Biol*, 1967; **26**: 329–46.

47. Mankin AS. Pactamycin resistance mutations in functional sites of 16 S rRNA. *J Mol Biol*, 1997; **274**: 8–15.
48. Milligan RA, Unwin PN. Location of exit channel for nascent protein in 80S ribosome. *Nature*, 1986; **319**: 693–5.
49. Miskin R, Zamir A, Elson D. The inactivation and reactivation of ribosomal-peptidyl transferase of E. coli. *Biochem Biophys Res Commun*, 1968; **33**: 551–7.
50. Moazed D, Noller HF. Intermediate states in the movement of transfer RNA in the ribosome. *Nature*, 1989; **342**: 142–8.
51. Moazed D, Noller HF. Sites of interaction of the CCA end of peptidyl-tRNA with 23S rRNA. *Proc Natl Acad Sci USA*, 1991; **88**: 3725–8.
52. Moazed D, Samaha RR, Gualerzi C, Noller HF. Specific protection of 16 S rRNA by translational initiation factors. *J Mol Biol*, 1995; **248**: 207–10.
53. Monro RE, Celma ML, Vazquez D. Action of sparsomycin on ribosome-catalysed peptidyl transfer. *Nature*, 1969; **222**: 356–8.
54. Monro RE, Cerna J, Marcker KA. Ribosome-catalyzed peptidyl transfer: substrate specificity at the P-site. *Proc Natl Acad Sci USA*, 1968; **61**: 1042–9.
55. Mueller F, Sommer I, Baranov P, Matadeen R, Stoldt M, Wohnert J, Gorlach M, van Heel M, Brimacombe R. The 3D arrangement of the 23 S and 5 S rRNA in the Escherichia coli 50 S ribosomal subunit based on a cryo-electron microscopic reconstruction at 7.5 A resolution. *J Mol Biol*, 2000; **298**: 35–59.
56. Muessig J, Makowski I, von Bohlen K, Hansen H, Bartels KS, Wittmann HG, Yonath A. Crystals of wild-type, mutated, derivatized and complexed 50 S ribosomal subunits from Bacillus stearothermophilus suitable for X-ray analysis. *J Mol Biol*, 1989; **205**: 619–21.
57. Nakatogawa H, Ito K. The ribosomal exit tunnel functions as a discriminating gate. *Cell*, 2002; **108**: 629–36.
58. Nikulin A, EliseikinaI, Tishchenko S, Nevskaya N, Davydova N, Platonova O, Piendl W, Selmer M, Liljas A, Drygin D, Zimmermann R, Garber M, Nikonov S. *Nat Struct Biol* 2003; **6**:6
59. Nierhaus KH, Schulze H, Cooperman BS. Molecular mechanisms of the ribosomal peptidyl transferase center. *Biochem Int*, 1980; **1**: 185–192.
60. Nissen P, Hansen J, Ban N, Moore PB, Steitz TA. The structural basis of ribosome activity in peptide bond synthesis. *Science*, 2000; **289**: 920–30.
61. Noller HF, Hoffarth V, Zimniak L. Unusual resistance of peptidyl transferase to protein extraction procedures. *Science*, 1992; **256**: 1416–9.

62. Odom OW, Kramer G, Henderson AB, Pinphanichakarn P, Hardesty B. GTP hydrolysis during methionyl-tRNAf binding to 40 S ribosomal subunits and the site of edeine inhibition. *J Biol Chem*, 1978; **253**: 1807–16.
63. Odom OW, Picking WD, Hardesty B. Movement of tRNA but not the nascent peptide during peptide bond formation on ribosomes. *Biochemistry*, 1990; **29**: 10734–44.
64. Ofengand J, Bakin A. Mapping to nucleotide resolution of pseudouridine residues in large subunit ribosomal RNAs from representative eukaryotes, prokaryotes, archaebacteria, mitochondria and chloroplasts. *J Mol Biol*, 1997; **266**: 246–68.
65. Ogle JM, Brodersen DE, Clemons WM Jr, Tarry MJ, Carter AP, Ramakrishnan V. Recognition of cognate transfer RNA by the 30S ribosomal subunit. *Science*, 2001; **292**: 897–902.
66. Pape T, Wintermeyer W, Rodnina M. Induced fit in initial selection and proofreading of aminoacyl-tRNA on the ribosome. *Embo J*, 1999; **18**: 3800–7.
67. Penczek P, Ban N, Grassucci RA, Agrawal RK, Frank J. Haloarcula marismortui 50S Subunit-Complementarity of Electron Microscopy and X-Ray Crystallographic Information. *J Struct Biol*, 1999; **128**: 44–50.
68. Pestka S. Inhibitors of protein synthesis, Weissbach, H. New York, 1977.
69. Pioletti M, Schluenzen F, Harms J, Zarivach R, Gluhmann M, Avila H, Bashan A, Bartels H, Auerbach T, Jacobi C, Hartsch T, Yonath A, Franceschi F. Crystal structures of complexes of the small ribosomal subunit with tetracycline, edeine and IF3. *Embo J*, 2001; **20**: 1829–39.
70. Polacek N, Gaynor M, Yassin A, Mankin AS. Ribosomal peptidyl transferase can withstand mutations at the putative catalytic nucleotide. *Nature*, 2001; **411**: 498–501.
71. Porse BT, Garrett RA. Mapping important nucleotides in the peptidyl transferase centre of 23 S rRNA using a random mutagenesis approach. *J Mol Biol*, 1995; **249**: 1–10.
72. Porse BT, Kirillov SV, Awayez MJ, Ottenheijm HC, Garrett RA. Direct crosslinking of the antitumor antibiotic sparsomycin, and its derivatives, to A2602 in the peptidyl transferase center of 23S-like rRNA within ribosome-tRNA complexes. *Proc Natl Acad Sci USA*, 1999; **96**: 9003–8.
73. Rheinberger HJ, Sternbach H, Nierhaus KH. Three tRNA binding sites on Escherichia coli ribosomes. *Proc Natl Acad Sci USA*, 1981; **78**: 5310–4.

74. Rodriguez-Fonseca C, Amils R, Garrett RA. Fine structure of the peptidyl transferase centre on 23 S-like rRNAs deduced from chemical probing of antibiotic-ribosome complexes. *J Mol Biol*, 1995; **247**: 224–35.
75. Rodriguez-Fonseca C, Phan H, Long KS, Porse, BT, Kirillov, SV, Amils, R, Garrett, RA. Puromycin-rRNA interaction sites at the peptidyl transferase center. *RNA*, 2000; **6**: 744–54.
76. Sabatini DD, Blobel G. Controlled proteolysis of nascent polypeptides in rat liver cell fractions. II. Location of the polypeptides in rough microsomes. *J Cell Biol*, 1970; **45**: 146–57.
77. Samaha RR, Green R, Noller HF. A base pair between tRNA and 23S rRNA in the peptidyl transferase centre of the ribosome. *Nature*, 1995; **377**: 309–14.
78. Sarker S, Rudd KE, Oliver D. Revised translation start site for secM defines an atypical signal peptide that regulates Escherichia coli secA expression. *J Bacteriol*, 2000; **182**: 5592–5.
79. Schluenzen F, Tocilj A, Zarivach R, Harms J, Gluehmann M, Janell D, Bashan A, Bartels H, Agmon I, Franceschi F, Yonath A. Structure of functionally activated small ribosomal subunit at 3.3 angstroms resolution. *Cell*, 2000; **102**: 615–23.
80. Schluenzen F, Zarivach R, Harms J, Bashan A, Tocilj A, Albrecht R, Yonath A, Franceschi F. Structural basis for the interaction of antibiotics with the peptidyl transferase centre in eubacteria. *Nature*, 2001; **413**: 814–21.
81. Schluenzen F, Harms J, Franceschi F, Hansen HAS, Bartels H, Zarivach R and Yonath A. Structural basis for the antibiotic activity of ketolides and azalides, *Structure*, 2003;**11**:329
82. Schmeing TM, Seila AC, Hansen JL, Freeborn B, Soukup JK, Scaringe SA, Strobel SA, Moore PB, Steitz TA. A pre-translocational intermediate in protein synthesis observed in crystals of enzymatically active 50S subunits. *Nat Struct Biol*, 2002; **9**: 225–30.
83. Shevack A, Gewitz HS, Hennemann B, Yonath A, Wittmann HG. Characterization and crystallization of ribosomal particles from Halobacterium marismortui. *FEBS Lett*, 1985; **184**: 68–71.
84. Smith JD, Traut RR, GM B, Monro RE. Action of puromycin in polyadenylic acid-directed polylysine synthesis. *J Mol Biol*, 1965; **13**: 617–628.
85. Spahn CM, Prescott CD. Throwing a spanner in the works: antibiotics and the translation apparatus. *J Mol Med*, 1996; **74**: 423–39.

86. Stark H, Orlova EV, Rinke-Appel J, Junke N, Mueller F, Rodnina M, Wintermeyer W, Brimacombe R, van Heel M. Arrangement of tRNAs in pre- and posttranslocational ribosomes revealed by electron cryomicroscopy. *Cell*, 1997; **88**: 19–28.
87. Stoffler G, Stoffler-Meilicke M. Immunoelectron microscopy of ribosomes. *Annu Rev Biophys Bioeng*, 1984; **13**: 303–30.
88. Stroud RM, Walter P. Signal sequence recognition and protein targeting. *Curr Opin Struct Biol*, 1999; **9**: 754–9.
89. Tenson T, Ehrenberg M. Regulatory nascent peptides in the ribosomal tunnel. *Cell*, 2002; **108**: 591–4.
90. Tenson T, Mankin AS. Short peptides conferring resistance to macrolide antibiotics. *Peptides*, 2001; **22**: 1661–8.
91. Thompson J, Kim DF, O'Connor M, Lieberman KR, Bayfield MA, Gregory ST, Green R, Noller HF, Dahlberg AE. Analysis of mutations at residues A2451 and G2447 of 23S rRNA in the peptidyltransferase active site of the 50S ribosomal subunit. *Proc Natl Acad Sci USA*, 2001; **98**: 9002–7.
92. Tocilj A, Schlunzen F, Janell D, Gluhmann M, Hansen HA, Harms J, Bashan A, Bartels H, Agmon I, Franceschi F, Yonath A. The small ribosomal subunit from Thermus thermophilus at 4.5 A resolution: pattern fittings and the identification of a functional site. *Proc Natl Acad Sci USA*, 1999; **96**: 14252–7.
93. Trakhanov SD, Yusupov MM, Agalarov SC, Garber MB, Ryazantsev SN, Tischenko SV, Shirokov VA. Crystallization of 70S Ribosomes and 30S Ribosomal Subunits from Thermus Thermophilus. *FEBS Lett*, 1987; **220**: 319–22.
94. Traut RR, Monr RE. The puromycin reaction and its relationship to protein synthesis. *J Mol Biol*, 1964; **10**: 63–72.
95. Unge J, berg A, Al-Kharadaghi S, Nikulin A, Nikonov S, Davydova N, Nevskaya N, Garber M, Liljas A. The crystal structure of ribosomal protein L22 from Thermus thermophilus: insights into the mechanism of erythromycin resistance. *Structure*, 1998; **6**: 1577–86.
96. Vazquez D. Inhibitors of protein biosynthesis. *Mol Biol Biochem Biophys*, 1979; **30**: 1–312.
97. Vogel Z, Vogel T, Zamir A, Elson D. Correlation between the peptidyl transferase activity of the 50 s ribosomal subunit and the ability of the subunit to interact with antibiotics. *J Mol Biol*, 1971; **60**: 339–46.
98. Volkmann N, Hottentrager S, Hansen HA, Zaytzev-Bashan A, Sharon R, Berkovitch-Yellin Z, Yonath A, Wittmann HG. Characterization and pre-

liminary crystallographic studies on large ribosomal subunits from Thermus thermophilus. *J Mol Biol*, 1990; **216**: 239–41.

99. von Bohlen K, Makowski I, Hansen HA, Bartels H, Berkovitch-Yellin Z, Zaytzev-Bashan A, Meyer S, Paulke C, Franceschi F, Yonath A. Characterization and preliminary attempts for derivatization of crystals of large ribosomal subunits from Haloarcula marismortui diffracting to 3 A resolution. *J Mol Biol*, 1991; **222**: 11–5.
100. Walter P, Johnson AE. Signal sequence recognition and protein targeting to the endoplasmic reticulum membrane. *Annu Rev Cell Biol*, 1994; **10**: 87–119.
101. Weisblum B. Erythromycin resistance by ribosome modification. *Antimicrob Agents Chemother*, 1995; **39**: 577–85.
102. White O, Eisen JA, Heidelberg JF, Hickey EK, Peterson JD, Dodson RJ, Haft DH, Gwinn ML, Nelson WC, Richardson DL, Moffat KS, Qin H, Jiang L, Pamphil W, Crosby M, Shen M, Vamathevan JJ, Lam P, McDonald L, Utterback T, Zalewski C, Makarova KS, Aravind L, Daly, MJ, Fraser CM, *et al*. Genome sequence of the radioresistant bacterium Deinococcus radiodurans R1. *Science*, 1999; **286**: 1571–7.
103. Wilson KS, Noller HF. Molecular movement inside the translational engine. *Cell*, 1998; **92**: 337–349.
104. Wimberly BT, Brodersen DE, Clemons WM Jr, Morgan-Warren RJ, Carter AP, Vonrhein C, Hartsch T, Ramakrishnan V. Structure of the 30S ribosomal subunit. *Nature*, 2000; 407: 327–39.
105. Woodcock J, Moazed D, Cannon M, Davies J, Noller HF. Interaction of antibiotics with A- and P-site-specific bases in 16S ribosomal RNA. *Embo J*, 1991; **10**: 3099–103.
106. Yonath A. The search and its outcome: high-resolution structures of ribosomal particles from mesophilic, thermophilic, and halophilic bacteria at various functional states. *Annu Rev Biophys Biomol Struct*, 2002; **31**: 257–73.
107. Yonath A, Bartunik HD, Bartels KS, Wittmann HG. Some X-ray diffraction patterns from single crystals of the large ribosomal subunit from Bacillus stearothermophilus. *J Mol Biol*, 1984; **177**: 201–6.
108. Yonath A, Glotz C, Gewitz HS, Bartels KS, von Bohlen K, Makowski I, Wittmann HG. Characterization of crystals of small ribosomal subunits. *J Mol Biol*, 1988; **203**: 831–4.

109. Yonath A, Leonard KR, Weinstein S, Wittmann HG. Approaches to the determination of the three-dimensional architecture of ribosomal particles. *Cold Spring Harb Symp Quant Biol*, 1987a; **52**: 729–41.
110. Yonath A, Leonard KR, Wittmann HG. A tunnel in the large ribosomal subunit revealed by three-dimensional image reconstruction. *Science*, 1987b; **236**: 813–6.
111. Yonath A, Muessig J, Tesche B, Lorenz S, Erdmann VA, Wittmann HG. Crystallization of the large ribosomal subunit from B. stearothermophilus. *Biochem Int*, 1980; **1**: 315–428.
112. Young JC, Andrews DW. The signal recognition particle receptor alpha subunit assembles co-translationally on the endoplasmic reticulum membrane during an mRNA-encoded translation pause in vitro. *Embo J*, 1996; **15**: 172–81.
113. Yusupov MM, Yusupova GZ, Baucom A, Lieberman, K, Earnest, TN, Cate, JH, Noller, HF. Crystal structure of the ribosome at 5.5 A resolution. *Science*, 2001; **292**: 883–96.
114. Zamir A, Miskin R, Elson D. Inactivation and reactivation of ribosomal subunits: amino acyl-transfer RNA binding activity of the 30 s subunit of Escherichia coli. *J Mol Biol*, 1971; **60**: 347–64.
115. Zamir A, Miskin R, Vogel Z, Elson D. The inactivation and reactivation of Escherichia coli ribosomes. *Methods Enzymol*, 1974; **30**: 406–26.
116. Zarivach R, Bashan A, Schluenzen F, Harms J, Pioletti M, Franceschi F, Yonath A. Initiation and inhibition of protein biosynthesis - studies at high resolution. Curr Protein Peptid Sci, 2002; **3**: 55–65.